International Refereed Journal of Engineering and Science (IRJES)
ISSN (Online) 2319-183X, (Print) 2319-1821
Volume 5, Issue 12 (December 2016), PP.20-31

Influence of Radiation Absorption, Viscous and Joules dissipation on MHD free Convection Chemically Reactive and Radiative Flow in a Moving Inclined Porous Plate with Temperature Dependent Heat Source

K.S. Balamurugan[1], J.L. Ramaprasad[2], Dharmaiah Gurram[3]and V.C.C. Raju[4]
[1]R.V.R & J.C College Of Engineering, Department Of Mathematics, Guntur Andhra Pradesh, India
[2]Department Of Mathematics, PB Siddhartha College Of Arts And Science, Vijayawada Andhra Pradesh, India
[3]Narasaraopeta Engineering College, Department Of Mathematics, Narasaraopet Andhra Pradesh, India
[4]Department Of Mathematics, University Of Botswana, Gaborone, Botswana

Abstract: Heat and Mass transfer properties on MHD boundary layer flow of a viscous, incompressible, free convective, chemically reactive, radiative and electrically conducting fluid on a moving inclined heated porous plate in the presence of radiation absorption, temperature dependent heat source and joule heating is analyzed. The non-linear coupled partial differential equations are solved by perturbation technique. The impact of different pertinent parameters on velocity, temperature and concentration distribution have been studied and explored with the help of graphs. Further, the results of the skin friction coefficient and dimensionless rate of heat and mass transfer at the plate are also presented.
Keywords: Viscous dissipation, Joules dissipation,chemicalreaction,inclinedplate,radiation absorption.

I. INTRODUCTION

The convective heat and mass transfer flows in an inclined porous plate find a number of applications in many branches of science and technology like chemical industry, cooling of nuclear reactors, MHD power generators, geothermal energy extractions processes, petroleum engineering etc. Convective heat and mass transfer flows in the presence of various physical properties for the cases of horizontal and vertical flat plates have been attracting the attention of many researchers now a days[1]–[14]. However, the boundary layer flows adjacent to inclined plates or wedges have received less attention.

For the problem of coupled heat and mass transfer in MHD free convection, the effect of both viscous dissipation and Ohmic heating are not studied in the above investigations. However, it is more realistic to include these two effects to explore the impact of the magnetic field on the thermal transport in the boundary layer. With this awareness, the effect of Ohmic heating on the MHD free convection heat transfer has been examined for a Newtonian fluid by Hossain [15]. Hossain and Gorla [16] studied Joule heating effect on magnetohydrodynamic mixed convection boundary layer flow, to investigate the mixed convection flow of an electrically conducting and viscous incompressible fluid past an isothermal vertical surface with Joule heating in the presence of a uniform transverse magnetic field fixed relative to the surface. It was assumed that the electrical conductivity of the fluid varies linearly with the transverse velocity component. Beg et al. [17] solved magnetohydrodynamic Hartmann–Couette flow and heat transfer in a Darcian channel with Hall current, ion slip, viscous and Joule heating effects. Chen [18] studied the problem of combined heat and mass transfer of an electrically conducting fluid in MHD natural convection, adjacent to a vertical surface with Ohmic heating. Reddy et al. [19] considered thermo diffusion and chemical effects with simultaneous thermal and mass diffusion in MHD mixed convection flow with Ohmic heating. Sibanda and Makinde [20] proceeded on steady MHD flow and heat transfer past a rotating disk in a porous medium with Ohmic heating and viscous dissipation. Mixed convection of Non- Newtonian fluids from a vertical plate embedded in a porous medium is studied by Wang et al. [21]. Viscous and Joule heating effects on non-Darcy MHD natural convection flow over a permeable sphere in porous media with internal heat generation was considered by Yih [22]. Choudhary and Das [23] examined on Mixed Convective visco-elastic MHD flow with Ohmic heating.

Motivated by the above studies, in this manuscript an attempt is made to investigate the effects of radiation absorption, temperature dependent heat source, viscous dissipation and Joule heating effects on a radiative and reactive, mixed convection MHD flow of a viscous, incompressible, electrically conducting and Newtonian fluid on a moving inclined heated porous plate. This is an extension to the work of C.Veeresh et al. [24], which has the novelty in studying Radiation absorption in the energy equation.

II. MATHEMATICAL FORMULATION

Consider a free convective laminar boundary layer flow of a viscous incompressible electrically conducting, chemically reactive, radiative and heat absorbing fluid past a semi-infinite moving permeable plate inclined at an angle α a in vertical direction embedded in a uniform porous medium, which is subject to thermal and concentration buoyancy effects along with Joule's dissipation and temperature dependent heat source. The temperature of the wall is maintained $T_w$and concentration $C_w$which is higher than the ambient temperature $T_\infty$and concentration C_∞respectively. Also it is assumed that there exists a homogeneous chemical reaction of first order with rate constant between the diffusing species and the fluid.

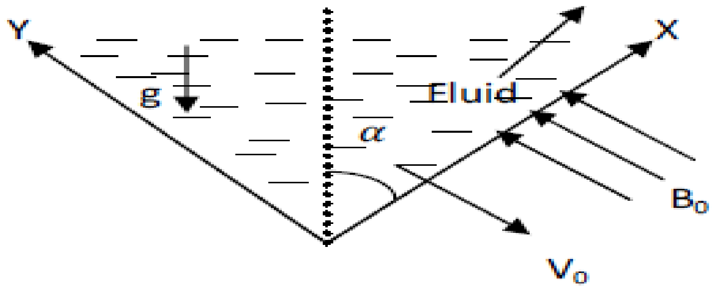

Physical Model

With these physical considerations, the equations governing the fluid in Cartesian frame of reference are given below.

$$\frac{\partial v}{\partial y} = 0 \quad \Rightarrow \quad v^* = -V_0 \tag{1}$$

Momentum Equation

$$\rho v^* \frac{\partial u^*}{\partial y^*} = \mu \frac{\partial^2 u^*}{\partial y^{*2}} - \frac{\mu}{K} u^* - \sigma B_0^2 u^* + \rho g \cos\alpha \ \beta_T (T^* - T_\infty) + \rho g \cos\alpha \ \beta_C (C^* - C_\infty) \tag{2}$$

Energy Equation

$$\rho C_p v^* \frac{\partial T^*}{\partial y^*} = \alpha_1 \frac{\partial^2 T^*}{\partial y^{*2}} + \mu \left(\frac{\partial u^*}{\partial y^*} \right)^2 - \frac{\partial q_r^*}{\partial y^*} + \sigma B_0^2 u^{*2} - Q_0 \frac{\partial}{\partial y^*} (T^* - T_\infty) + R_A (C^* - C_\infty) \tag{3}$$

Concentration Equation

$$v^* \frac{\partial C^*}{\partial y^*} = D \frac{\partial^2 C^*}{\partial y^{*2}} - R(C^* - C_\infty) \tag{4}$$

The radiative heat flux $\frac{\partial q_r^*}{\partial y^*} = 4(T^* - T_\infty) I^{'}$ (5)

where

$I^{'} = \int_0^\infty K_{\lambda w} \frac{\partial e_{b\lambda}}{\partial T^*} d\lambda, \quad K_{\lambda w}$ is the absorption coefficient at the wall and $e_{b\lambda}$ is Plank's function.

Under these assumptions the appropriate boundary conditions for velocity, temperature and concentration fields are defined as

$$u^* = u_p^*, \quad T^* = T_w, \quad C^* = C_w \qquad at \quad y = 0 \tag{6}$$

$$u^* \to 0, \quad T^* \to T_\infty, \quad C^* \to C_\infty \qquad as \quad y \to \infty \tag{7}$$

Introducing the following non-dimensional quantities

$$u=\frac{u^*}{v_0},\upsilon=\frac{\mu}{\rho},R_1=\frac{\upsilon(C_w-C_\infty)R_A}{v_0^2\rho C_p(T_w-T_\infty)},y=\frac{v_0y^*}{\upsilon},u_p=\frac{u_p^*}{v_0},M^2=\frac{B_0^2\upsilon^2\sigma}{v_0^2\mu},K=\frac{K^*v_0^2}{\upsilon^2},$$

$$\theta=\frac{T^*-T_\infty}{T_w-T_\infty},C=\frac{C^*-C_\infty}{C_w-C_\infty},Sc=\frac{\upsilon}{d},\gamma=\frac{R\upsilon}{v_0^2},\Pr=\frac{\mu Cp}{\alpha_1},H=\frac{Q_0}{\rho C_pv_0^3},F=\frac{4\upsilon I'}{\rho C_pv_0^2},$$

$$Ec=\frac{v_0^2}{C_p(T_w-T_\infty)},Gr=\frac{\rho g\beta_T\upsilon^2(T_w-T_\infty)}{v_0^3\mu},Gc=\frac{\rho g\beta_C\upsilon^2(C_w-C_\infty)}{v_0^3\mu} \tag{8}$$

where the parameters are Grashof number Gr, modified Grashof number Gm, angle of inclination α, radiation parameter F, Schmidt number Sc, chemical reaction parameter γ, Hartmann number M, temperature dependent heat source parameter H, porosity parameter K, Prandtl number Pr, Schmidt number Sc and Radiation Absorption parameter R_1.

The basic field equations (2) – (4), can be expressed in non-dimensional form as

$$\frac{\partial^2u}{\partial y^2}+\frac{\partial u}{\partial y}-\left(M+\frac{1}{K}\right)u=-Gr\theta\cos\alpha-GmC\cos\alpha \tag{9}$$

$$\frac{\partial^2\theta}{\partial y^2}+\Pr(1-H)\frac{\partial\theta}{\partial y}+\Pr Ec\left(\frac{\partial u}{\partial y}\right)^2+\Pr EcM^2u^2=\Pr F\theta-\Pr R_1C \tag{10}$$

$$\frac{\partial^2C}{\partial y^2}+Sc\frac{\partial C}{\partial y}-Sc\,\gamma\,C=0 \tag{11}$$

The corresponding boundary conditions in non-dimensional form are:

$$u=u_p^*,\theta=1,C=1\quad at\quad y=0 \tag{12}$$

$$u\to0,\quad\theta\to0,\quad C\to0\quad as\quad y\to\infty \tag{13}$$

III. METHOD OF SOLUTION

The set of partial differential equations (9) – (11) cannot be solved in closed form. However, they can be solved analytically after reducing them into a set of ordinary differential equations by taking the expressions for velocity *u(y)*, temperature *θ(y)* and concentration *C(y)* in dimensionless form as follows:

$$u(y)=u_0(y)+Ec\,u_1(y)+O(E_c^2) \tag{14}$$

$$\theta(y)=\theta_0(y)+Ec\theta_1(y)+O(E_c^2) \tag{15}$$

$$C(y)=C_0(y)+C_1(y)+O(E_c^2) \tag{16}$$

Substituting (14) – (16) in (9) – (11) and equating the coefficients of zeroth order of Eckert number(constants), equating the coefficients of the first order of Eckert number, and neglecting the higher order of $O(E_c^2)$ and simplifying to get the following set of equations

$$u_0''+u_0'-pu=-Gr\theta_0\cos\alpha-GmC_0\cos\alpha \tag{17}$$

$$\theta_0''+\Pr(1-H)\theta_0'-\Pr F\theta_0=-\Pr R_1C_0 \tag{18}$$

$$C_0''+ScC_0'-Sc\,\gamma\,C_0=0 \tag{19}$$

$$u_1''+u_1'-pu_1=-Gr\theta_1\cos\alpha-GmC_1\cos\alpha \tag{20}$$

$$\theta_1''+pr(1-H)\theta_1'-\Pr F\theta_1=-\Pr u_0'^2-\Pr M^2u_0^2-\Pr R_1C_1 \tag{21}$$

$$C_1''+ScC_1'-Sc\,\gamma\,C_1=0 \tag{22}$$

where prime denotes ordinary differentiation with respect to ‘y’ and $p = M^2 + \frac{1}{K}$

The corresponding boundary conditions are:

$$u_0 = u_p, u_1 = 0, \theta_0 = 1, \theta_1 = 0, C_0 = 1, C_1 = 0 \qquad at \quad y = 0 \tag{23}$$

$$u_0 \to 0, u_1 \to 0, \theta_0 \to 0, \theta_1 \to 0, C_0 \to 0, C_1 \to 0 \qquad as \quad y \to \infty \tag{24}$$

Using boundary conditions (23) and (24), the solutions of (17) – (22), we obtain the following expressions for velocity, temperature and concentration.

$$u_0 = z_5 e^{-m_5 y} - z_3 e^{-m_3 y} - z_4 e^{-m_1 y} \tag{25}$$

$$\theta_0 = z_2 e^{-m_3 y} + z_1 e^{-m_1 y} \tag{26}$$

$$C_0 = e^{-m_1 y} \tag{27}$$

$$u_1 = z_6 e^{-m_9 y} - z_7 e^{-m_7 y} + z_8 e^{-2m_5 y} + z_9 e^{-2m_3 y} + z_{10} e^{-2m_1 y} - z_{11} e^{-m_{10} y} + z_{12} e^{-m_{11} y} - z_{13} e^{-m_{12} y} \tag{28}$$

$$\theta_1 = z_{14} e^{-m_7 y} - z_{15} e^{-2m_5 y} - z_{16} e^{-2m_3 y} - z_{17} e^{-2m_1 y} + z_{18} e^{-m_{13} y} - z_{19} e^{-m_{14} y} + z_{20} e^{-m_{15} y} \tag{29}$$

$$C_1 = 0 \tag{30}$$

Substituting the above solutions (25) – (30) in (14) – (16), we get the final form of Velocity, Temperature, Concentration distributions in the boundary layer as follows

$$u(y) = \left[z_5 e^{-m_5 y} - z_3 e^{-m_3 y} - z_4 e^{-m_1 y} \right] + Ec \begin{bmatrix} z_6 e^{-m_9 y} - z_7 e^{-m_7 y} + z_8 e^{-2m_5 y} + z_9 e^{-2m_3 y} + z_{10} e^{-2m_1 y} \\ - z_{11} e^{-m_{10} y} + z_{12} e^{-m_{11} y} - z_{13} e^{-m_{12} y} \end{bmatrix} \tag{31}$$

$$\theta(y) = \left[z_2 e^{-m_3 y} + z_1 e^{-m_1 y} \right] + Ec \begin{bmatrix} z_{14} e^{-m_7 y} - z_{15} e^{-2m_5 y} - z_{16} e^{-2m_3 y} - z_{17} e^{-2m_1 y} \\ + z_{18} e^{-m_{13} y} - z_{19} e^{-m_{14} y} + z_{20} e^{-m_{15} y} \end{bmatrix} \tag{32}$$

$$C(y) = e^{-m_1 y} \tag{33}$$

The physical quantities of interest are the wall shear stress τ_w is given by

$$\tau_w = \mu \left. \frac{\partial u^*}{\partial y^*} \right|_{y^*=0} = \rho v_0^2 u'(0)$$

The local skin friction factor τ is given by $\tau = \frac{\tau_w}{\rho v_0^2} = u'(0)$ (34)

The local surface heat flux is given by: $q_w = -\kappa \left. \frac{\partial T^*}{\partial y^*} \right|_{y^*=0}$

The local Nusselt number $Nu_x = \frac{q_w}{(T_w - T_\infty)}$ can be written as $\frac{Nu_x}{\mathrm{Re}_x} = -\left. \frac{\partial \theta}{\partial y} \right|_{y=0}$ (35)

The local surface mass flux is given by

$$\frac{Sh_x}{\mathrm{Re}_x} = -\left. \frac{\partial C}{\partial y} \right|_{y=0} = -m_1 \tag{36}$$

where $\mathrm{Re}_x = \dfrac{v_0 x}{\upsilon}$ is the local Reynolds number.

IV. RESULTS AND DISCUSSIONS

The present study considers the effects of radiation absorption R_1 and chemical reaction γ on transient free convection flow of heat and mass transfer in MHD free convective Joule heating and radiative flow in a moving inclined porous plate with temperature dependent heat source. Solutions for velocity, temperature and concentration field are obtained by using perturbation technique with $\gamma = 0.1$, Ec = 0.01, Sc = 0.60, Pr = 0.71, M = 2.0, K = 0.5, Gm = 2.0, Gr = 4.0, $\alpha = \pi/6$, H = 1.0, F =1.0, R = 0.01, $u_p = 0.1$ and therefore all the graphs corresponds to these unless specifically indicated on the appropriate graph. The effects of various parameters like Grashof number Gr, modified Grashof number Gm, angle of inclination α, radiation parameter F, Schmidt number Sc, chemical reaction parameter γ, Hartmann number M, temperature dependent heat source parameter H, porosity parameter K, Prandtl number Pr, Schmidt number Sc and Radiation Absorption parameter R_1, on velocity, temperature and concentration have been studied analytically and effects are executed with the help of figures. Also the behavior of skin-friction, rate of heat transfer and rate of mass transfer with respect to various parameters has been studied and results were presented in tables.

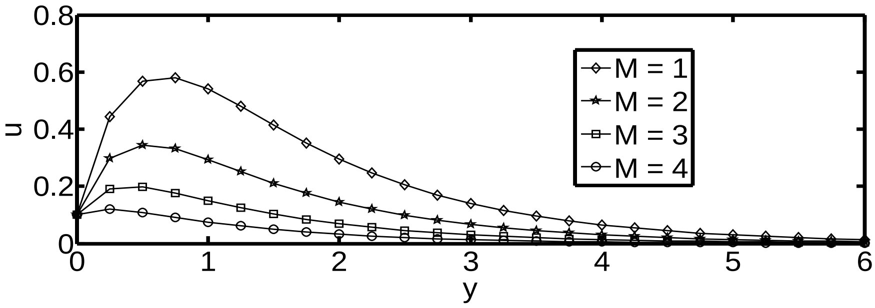

Figure 1: Velocity profiles for different values of Hartmann number M

Figure 1 exhibits the effect of Hartmann number (M). It is noticed that as the values of M increase velocity profiles gradually decrease. The effect of magnetic field is more prominent at the point of peak value i.e. the peak value drastically decreases with increase in the magnetic field, because the presence of magnetic field in an electrically conducting fluid introduces a force called the Lorentz force, which acts against the flow if the magnetic field is applied in the normal direction, as in the present problem. This type of resisting force slows down the fluid velocity as shown in this figure.Figure 2 shows the velocity profile for different values of porosity parameter (K). As K increases velocity also increases. Figure 3 shows the effects of angle of inclination (α) on velocity profile. We observed that the velocity decreases for increasing the angle of inclination α. Figure 4 depicts the effects of Grashof number (Gr) on velocity profile.From this figure it is noticed that the velocity decreases as Grashof number increases. Figure5 represents typical velocity profiles in the boundary layer for various values of the modified Grashof number. The velocity distribution attains a distinctive maximum value in the vicinity of the plate surface and then decrease properly to approach the free stream value. As expected, the fluid velocity increases and the peak value more distinctive due to increase in the concentration buoyancy effects represented by modified Grashof number. This is evident with the increase in the value of velocity as modified Grashof number increases.

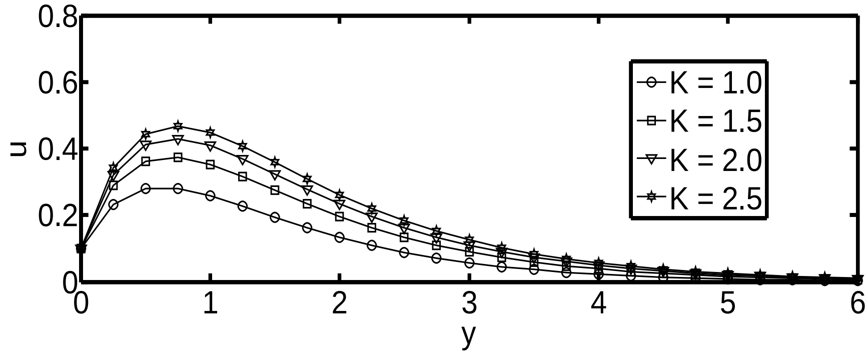

Figure 2: Velocity profiles for different values of porosity parameter K

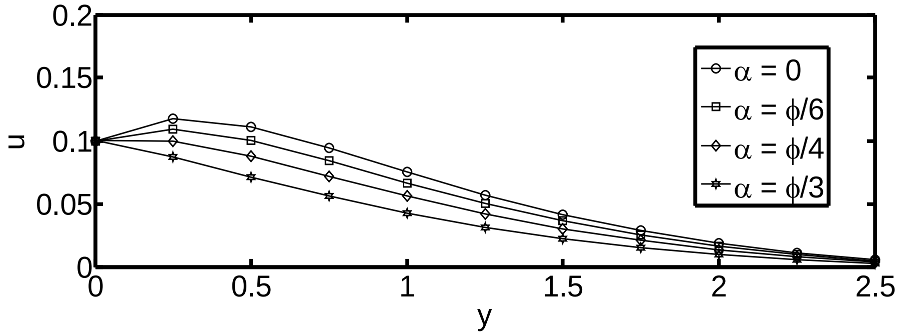

Figure 3: Velocity profiles for different values of angle of inclination α

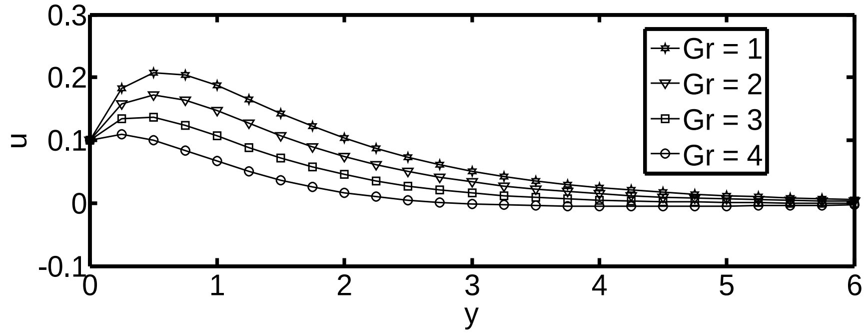

Figure 4: Velocity profiles for different values of Grashof number Gr

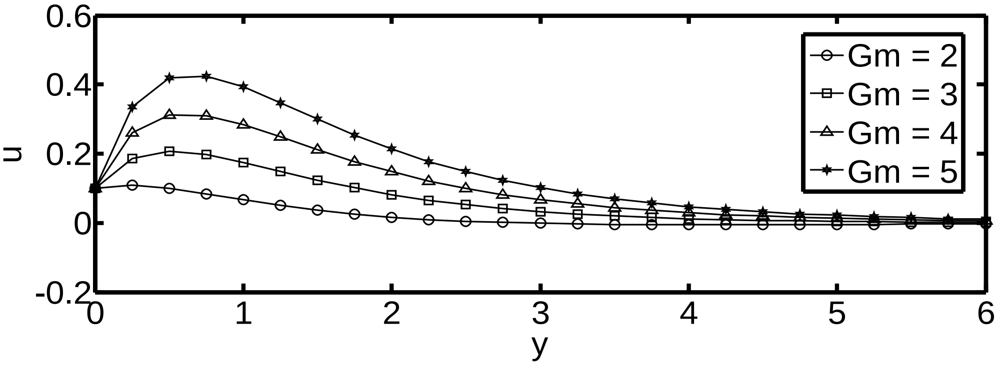

Figure 5: Velocity profiles for different values of Gm

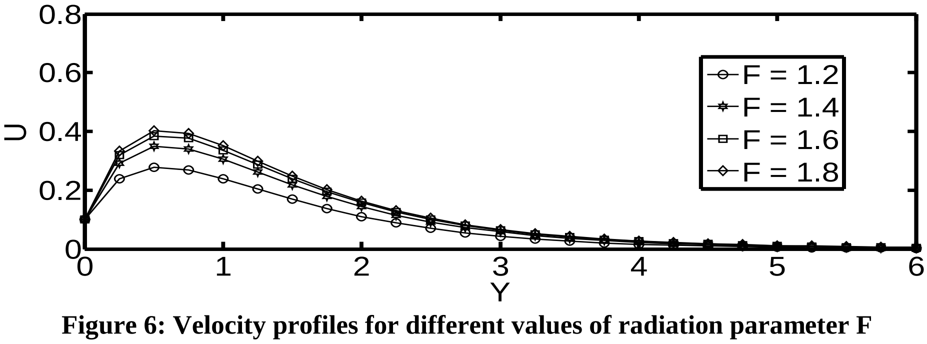

Figure 6: Velocity profiles for different values of radiation parameter F

Figure 6 shows the velocity profiles for different values of the radiation parameter (F). It is clear that as radiation parameter increases the peak values of the velocity tend to increase. For different values of the Schmidt number (Sc) the velocity profiles are plotted in Figure 7. It is obvious that an increase in the Schmidt number results in decrease in the velocity within the boundary layer. Figure 8 illustrates the velocity profiles for different values of Prandtlnumber. It is observed that the velocity decreasesfor an increasing the Prandtl number. The influence of radiation absorptionparameter (R_1) on the velocity profile is shown in Figure 9. It is observed that an increase in the radiation absorption parameter causes to decrease the fluid velocity.

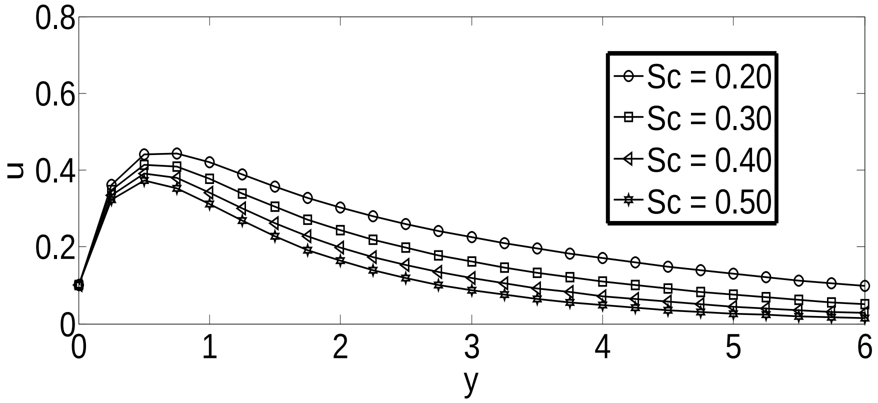

Figure 7: Velocity profiles for different values of Schmidt number Sc

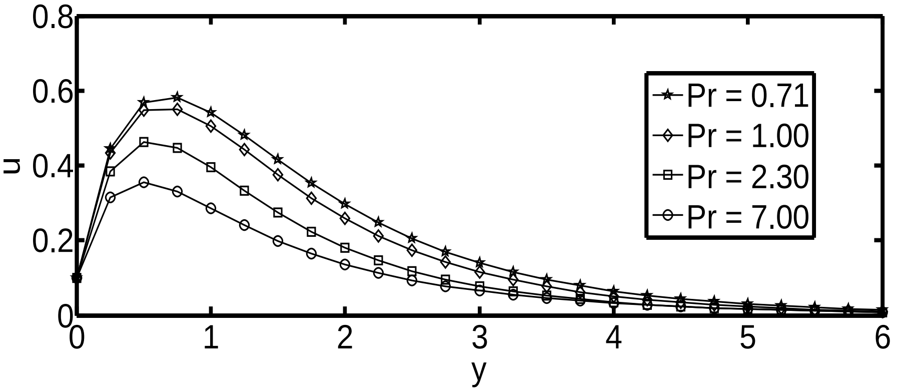

Figure 8: Velocity profiles for different values of Prandtl number Pr

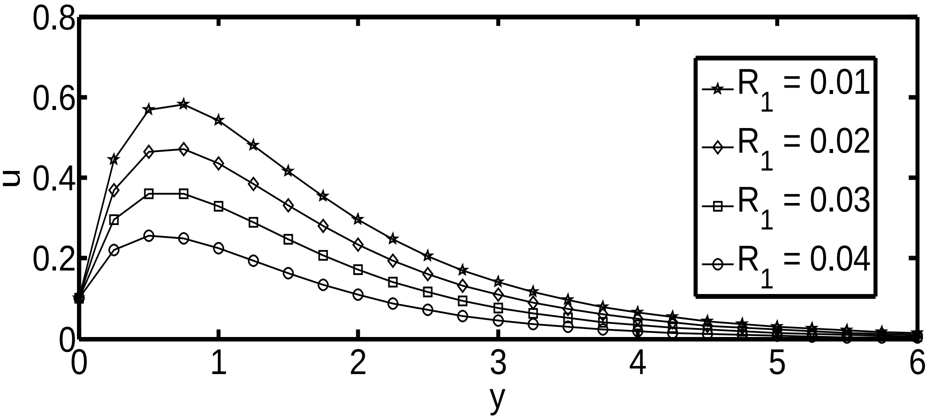

Figure 9: Velocity profiles for different values of Radiation Absorption parameter R_1

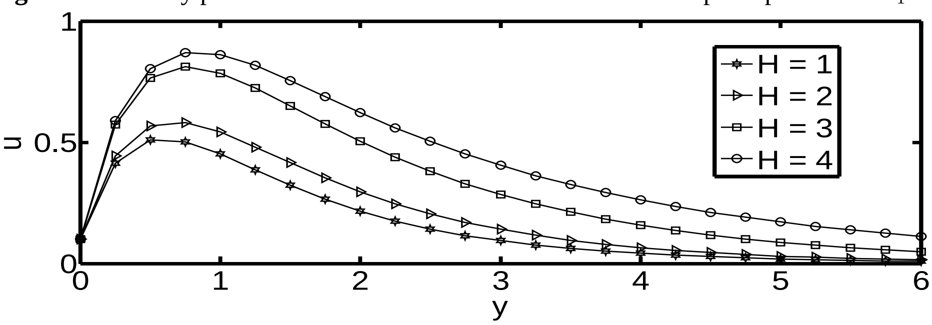

Figure 10: Velocity profiles for different values of heat source parameter H.

Velocity profiles for different values of heat source parameter (H) are shown in Figure 10. As H increases velocity distribution increases. Figure 11 exhibits the effect of radiation parameter (F) on temperature profile. It is seen that F increases as temperature decreases. Temperature profiles for different values of

Radiation Absorption parameter (R_1) are shown in Figure 12. It is noticed that an increase in the radiation absorption parameter causes to increase the fluid temperature. Figure 13 illustrates the temperature profiles for different values of Prandtlnumber. It is observed that the temperature decreases as Prandtl numberincreases. The reason is that smaller values of Prandtl number are equivalent to increase in the thermal conductivity of the fluid and therefore heat is able to diffuse away from the heated surface more rapidly for higher values of Prandtl number. Hence in the case of smaller Prandtl number the thermal boundary layer is thicker and the rate of heat transfer is reduced. Effect of H on temperature is presented in Figure 14. From this figure it is noticed that temperature increases as H increases. For different values of the Schmidt number the temperature profiles are plotted in Figure 15. It is obvious that an increase in the Schmidt number results in decrease in the temperature within the boundary layer.

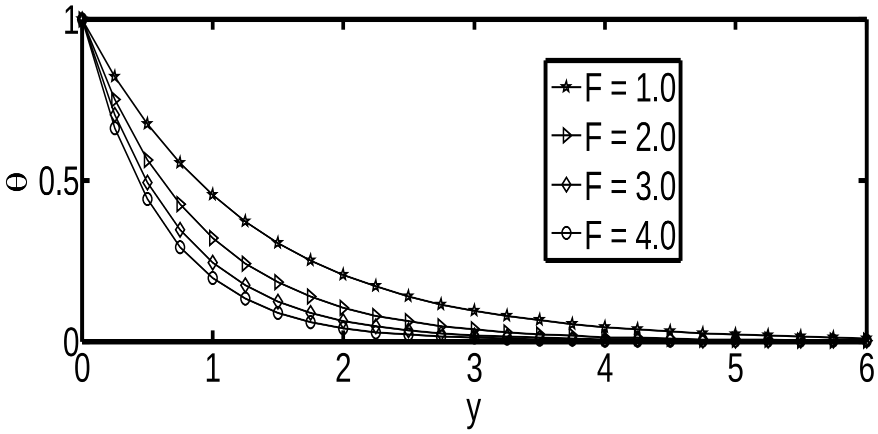

Figure 11: Temperature profiles for different values of radiation parameter F

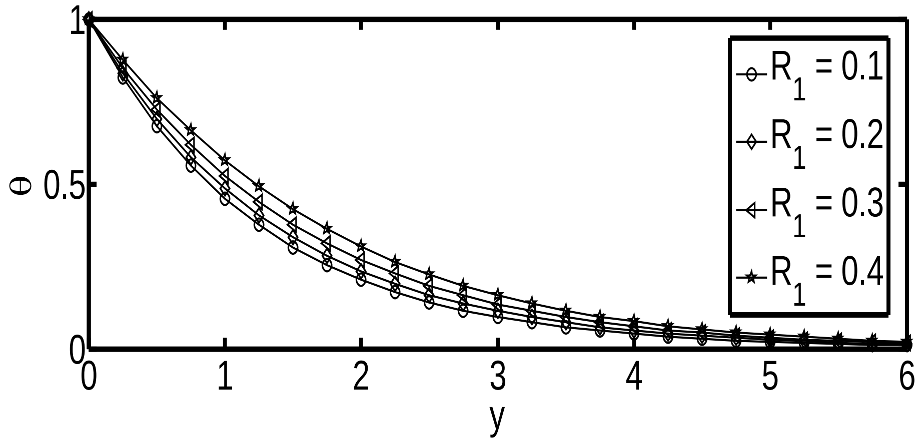

Figure 12: Temperature profiles for different values of R_1.

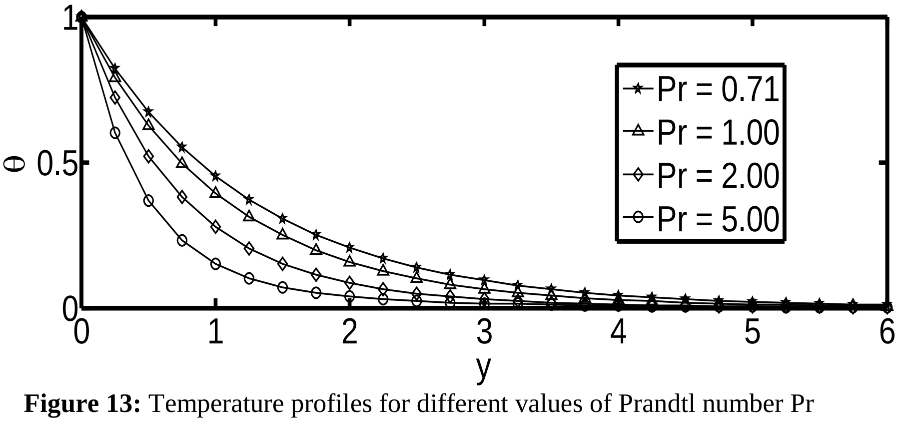

Figure 13: Temperature profiles for different values of Prandtl number Pr

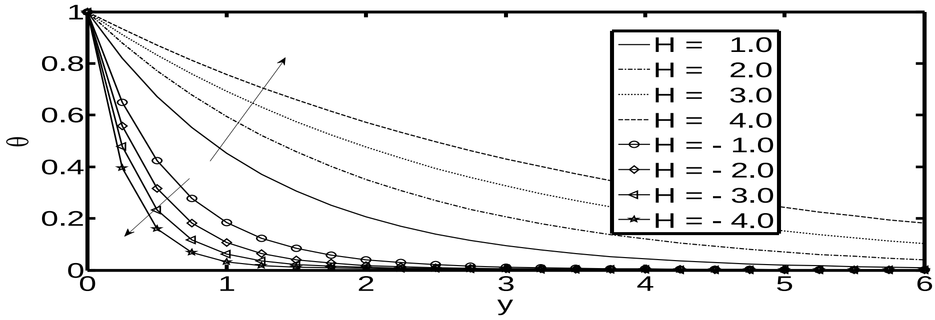

Figure 14: Temperature profiles for different values of heat source parameter H.

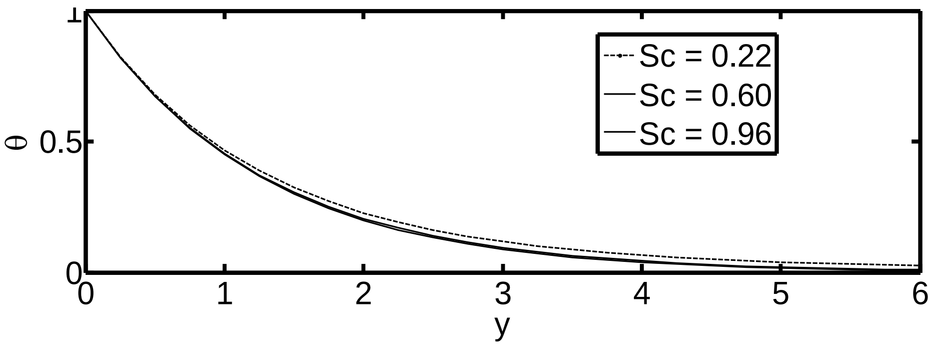

Figure 15: Temperature profiles for different values of Schmidt number Sc.

Figure 16 illustrates the behavior concentration for different values of chemical reaction parameter γ. It is observed that an increase γ leads to a decrease in the values of concentration. Figure 17 displays the effect of Schmidt number *Sc* on the concentration profiles. It is noticed that as the Schmidt number increases the concentration decreases.

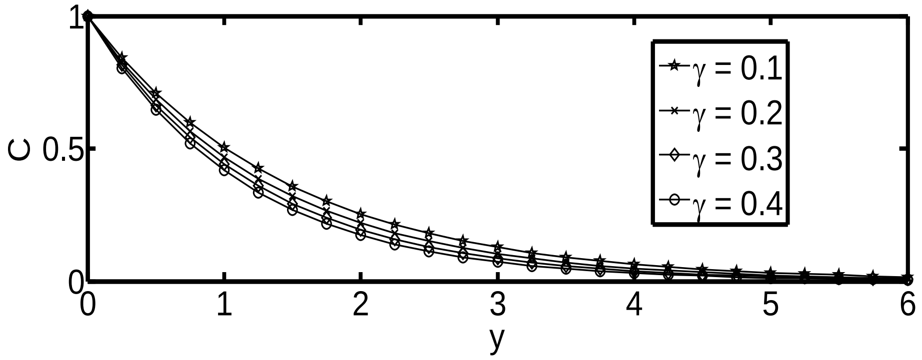

Figure 16: Concentration profiles for different values of Chemical reaction parameter γ

.

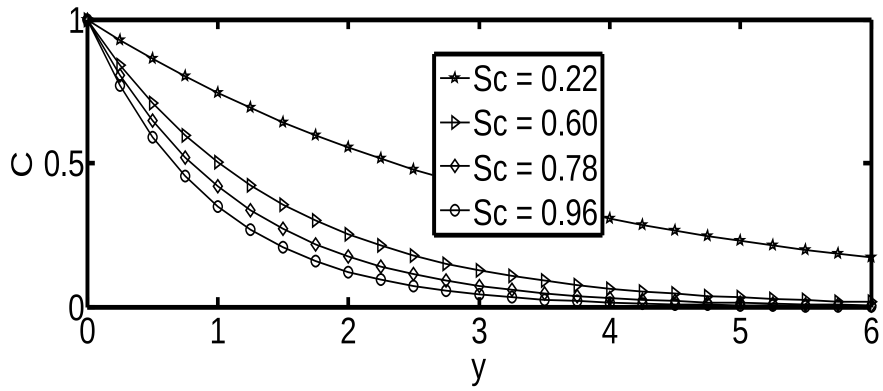

Figure 17: Concentration profiles for different values of Schmidt number Sc.

From Table 1, we conclude that increasing of K, Gr, Gm will increase the skin-friction. Also increasing of M, α, F, Sc, Pr, R_1, H will decrease skin-friction. From Table 2, it is found that increasing of Pr, F will increase the Nusselt number. Also increasing of Sc, R_1, Hwill decrease the Nusselt number. From Table 2, we conclude that increasing of Sc, γ will decrease Sherwood number.

Table 1: The effects of Skin-friction coefficient

M	K	α	Gr	Gm	F	Sc	Pr	R_1	H	τ
1.0	0.5	π/6	4.0	2.0	1.0	0.60	7	0.01	1.0	1.4504
2.0	0.5	π/6	4.0	2.0	1.0	0.60	7	0.01	1.0	0.9979
2.0	**1.0**	π/6	4.0	2.0	1.0	0.60	7	0.01	1.0	1.1163
2.0	**1.5**	π/6	4.0	2.0	1.0	0.60	7	0.01	1.0	1.1613
2.0	0.5	**0**	4.0	2.0	1.0	0.60	7	0.01	1.0	1.1993
2.0	0.5	**π/4**	4.0	2.0	1.0	0.60	7	0.01	1.0	0.7593
2.0	0.5	π/6	**1.0**	2.0	1.0	0.60	7	0.01	1.0	0.5077
2.0	0.5	π/6	**2.0**	2.0	1.0	0.60	7	0.01	1.0	0.6710
2.0	0.5	π/6	4.0	**3.0**	1.0	0.60	7	0.01	1.0	1.3214
2.0	0.5	π/6	4.0	**4.0**	1.0	0.60	7	0.01	1.0	1.6452
2.0	0.5	π/6	4.0	2.0	**1.4**	0.60	7	0.01	1.0	0.9591
2.0	0.5	π/6	4.0	2.0	**1.6**	0.60	7	0.01	1.0	0.9439
2.0	0.5	π/6	4.0	2.0	**1.8**	0.60	7	0.01	1.0	0.9398
2.0	0.5	π/6	4.0	2.0	1.0	**0.22**	7	0.01	1.0	1.1004
2.0	0.5	π/6	4.0	2.0	1.0	**0.78**	7	0.01	1.0	0.9596
2.0	0.5	π/6	4.0	2.0	1.0	**0.96**	7	0.01	1.0	0.9256
2.0	0.5	π/6	4.0	2.0	1.0	0.60	**0.7**	0.01	1.0	1.2831
2.0	0.5	π/6	4.0	2.0	1.0	0.60	**1.7**	0.01	1.0	1.2693
2.0	0.5	π/6	4.0	2.0	1.0	0.60	**2.7**	0.01	1.0	1.1885
2.0	0.5	π/6	4.0	2.0	1.0	0.60	7	**0.02**	1.0	0.9037
2.0	0.5	π/6	4.0	2.0	1.0	0.60	7	**0.03**	1.0	0.8096
2.0	0.5	π/6	4.0	2.0	1.0	0.60	7	**0.04**	1.0	0.7155
2.0	0.5	π/6	4.0	2.0	1.0	0.60	7	0.01	**1.5**	1.2102
2.0	0.5	π/6	4.0	2.0	1.0	0.60	7	0.01	**2.0**	1.1673
2.0	0.5	π/6	4.0	2.0	1.0	0.60	7	0.01	**2.5**	2.6045

Table 2: The effects of Nusselt number

R_1	Pr	H	F	Sc	Nu
0.01	0.71	1.0	1.0	0.60	0.8539
0.02	0.71	1.0	1.0	0.60	0.8436
0.03	0.71	1.0	1.0	0.60	0.8346
0.01	**1.0**	1.0	1.0	0.60	1.0195
0.01	**2.0**	1.0	1.0	0.60	1.3193
0.01	**5.0**	1.0	1.0	0.60	2.3093
0.01	0.71	**2.0**	1.0	0.60	0.5834
0.01	0.71	**3.0**	1.0	0.60	0.4120
0.01	0.71	**4.0**	1.0	0.60	0.3123
0.01	0.71	1.0	**2.0**	0.60	1.2103
0.01	0.71	1.0	**3.0**	0.60	1.4475
0.01	0.71	1.0	**4.0**	0.60	1.6881
0.01	0.71	1.0	1.0	**0.22**	0.8615
0.01	0.71	1.0	1.0	**0.78**	0.8927
0.01	0.71	1.0	1.0	**0.96**	0.8573

Table 3: The effect of Sherwood number at the plate

γ	Sc	Sh
0.1	**0.22**	-0.2947
0.1	**0.60**	-0.6873
0.1	**0.78**	-0.8697
0.2	0.60	-0.7583
0.3	0.60	-0.8186
0.4	0.60	-0.8745

Conclusions

Some Of The Important Conclusions Of The Study Are As Follows:

1. Velocity increases with the increase of *K* and *F* and decreases with the increase of *M* and α .
2. Increase of *Gr*, R_1, *Pr* and *Sc* lead to decrease of velocity.
3. Temperature decreases with the increase of *F*,*Pr* and *Sc* and increases with the increase of R_1.
4. Concentration decreases as *Sc*and γ increases.
5. Sherwood number decreases as *Sc*and γ increases.

REFERENCES

[1]. Youn J. Kim, Unsteady MHD convective heat transfer past a semi-infinite vertical porous moving plate with variable suction, International Journal of Engineering Science, 38, 833-845, 2000.

[2]. A.G. Vijayakumar, S.V.K. Varma and K.S. Balamurugan, The effects of heat source and radiation on unsteady MHD free convective fluid flow embedded in a porous medium with time dependent suction, Far East Journal of Applied Mathematics, 61(2), 91-116, 2011.

[3]. S. Masthan Rao, K.S. Balamurugan and S.V.K. Varma, Chemical reaction effects on MHDfree convection flow through a porous medium bounded by an inclined surface, International Journal of Mathematics and Computer Applications Research, 3(3), 13-22, 2013.

[4]. S.E. Mahgoub, Forced convection heat transfer over a flat plate in aporous medium, Ain Shams Engineering Journal, 4, 605-613, 2013.

[5]. S. Masthan Rao, K.S. Balamurugan, S.V.K. Varma and V.C.C. Raju, Chemical reaction and hall effects on MHD convective flow along an infinite vertical porous plate with variable suction and heat absorption, Applications and Applied Mathematics International Journal, 8(1), 268-288, 2013.

[6]. J. Prakash, K.S. Balamurugan, S.V.K. Varma, Soret and Chemical reaction effects on a three dimensional MHD convective flow of dissipative fluid along an infinite vertical porous plate, Journal of Computational and Applied Research in Mechanical Engineering, 4(1), 19-42, 2014.

[7]. G.S. Seth, S. Sarkar and S.M. Hussain, Effects of hall current, radiation and rotation on natural convection heat and mass transfer flow past a moving vertical plate, Ain Shams Engineering Journal, 5, 485-503, 2014.

[8]. Ch.H.K. Gopal, K.S. Balamuruganand V.C.C. Raju, Effect of Maxwell fluid on unsteady hydro magnetic flow through a porous medium in a rotating parallel plate channel, Extensive Journal of Applied Sciences, 3(5), 182-193, 2014.

[9]. J. Prakash, K.S. Balamurugan, S.V.K. Varma, Thermo-diffusion and chemical reaction effects on MHD three dimensional free convective coquette flow, Walailak Journal of Science and Technology, 12(9), 805-830, 2015.

[10]. K.S. Balamurugan, S.V.K. Varma and V.C.C. Raju, Chemical reaction and Thermo-diffusion effects on MHD free convective flow past a moving vertical plate with a time dependent suction and heat source in a slip flow regime, International Journal of Engineering and Scientific Research, 3(7), 102-114, 2015.

[11]. Y. Sudharshan Reddy, S.V.K. Varma, K.S. Balamurugan and J.L. Ramaprasad, Chemical reaction and Radiation absorption effects on hydromagnetic free convection flow past a vertical plate with constant mass flux, Far East Journal of Mathematical Sciences, 98(2), 133-149, 2015.

[12]. K.S. Balamurugan, J.L. Ramaprasad and S.V.K. Varma, Unsteady MHD free convective flow past a moving vertical plate with time dependent suction and chemical reaction in a slip flow regime, Procedia Engineering, 127, 516-523, 2015.

[13]. Rajeswari Sheshadri and Shankar Rao Munjam, Mixed convection flow due to vertical plate in the presence of heat source and chemical reaction, Ain Shams Engineering Journal, 7, 671-682, 2016.

[14]. K.S. Balamurugan, Dharmaiah Gurram, S.V.K. Varma and V.C.C. Raju, MHD free convective flow past a semi-infinite permeable moving plate with heat absorption, International Journal of Engineering and Scientific Research, 4(8), 46-59, 2016.

[15]. M.A.Hossain,Viscous and Joule heating effects on MHD-free convection flow with variable plate Temperature, International Journal of Heat and Mass Transfer, 35(12), 3485–3487, 1992.

[16]. M.A. Hossain and R.S. Gorla, Joule heating effect on magnetohydrodynamic mixed convection boundary layer flow with variable electrical conductivity, International Journal of Numerical Methods for Heat & Fluid Flow, 23(2), 275 – 288, 2013.

[17]. O.A. Bég, J. Zueco and H.S. Takhar, Unsteady magnetohydrodynamic Hartmann–Couette flow and heat transfer in a Darcian channel with Hall current, ion slip, viscous and Joule heating effects: Network numerical solutions, Communications in nonlinear science and numerical simulation, 14(4), 1082-1097, 2009.

[18]. C.H. Chen, Combined heat and mass transfer in MHD free convection from a vertical surface with Ohmic heating and viscous dissipation, International journal of engineering science, 42(7), 699-713, 2004.

[19]. N.A. Reddy, S.V.K. Varma and M. C. Raju, Thermo diffusion and chemical effects with simultaneous thermal and mass diffusion in MHD mixed convection flow with Ohmic heating, Journal of Naval Architecture and Marine Engineering, 6, 84-93, 2009.

[20]. P. Sibanda and O.D. Makinde, On steady MHD flow and heat transfer past a rotating disk in a porous medium with Ohmic heating and viscous dissipation, International Journal of Numerical Methods for Heat & Fluid Flow, 20 (3), 269 - 285, 2010.

[21]. A. Wang, C. Tu and X. Zhang, Mixed convection of non-newtonian fluids from a vertical plate embedded in a porous medium, Acta Mechanica Cinica, 6 (3), 214-220, 1990.

[22]. K. A. Yih, Viscous and Joule heating effects on non-Darcy MHD natural convection flow over a permeable sphere in porous media with internal heat generation, International communications in heat and mass transfer, 27(4), 591-600, 2000.
[23]. R. Choudhary and S.K. Das, Mixed Convective visco elastic MHD flow with Ohmic heating, International Journal of computer applications, 68 (10), 7-13, 2013.
[24]. C. Veeresh, S.V.K.Varma and D.Praveena, Heat and Mass transfer in MHD free convection chemically reactive flow in amoving inclined porous plate with temperature dependent heat source and joule heating, International Journal of Management, Information Technology and Engineering, 3 (11), 63-74, 2015.